

Article

## Mass Transfer in a Rotating Packed Bed with Viscous Newtonian and Non-Newtonian Fluids

Yu-Shao Chen, Chia-Chang Lin, and Hwai-Shen Liu

*Ind. Eng. Chem. Res.*, **2005**, 44 (4), 1043-1051 • DOI: 10.1021/ie0499409

Downloaded from <http://pubs.acs.org> on November 23, 2008

### More About This Article

Additional resources and features associated with this article are available within the HTML version:

- Supporting Information
- Links to the 3 articles that cite this article, as of the time of this article download
- Access to high resolution figures
- Links to articles and content related to this article
- Copyright permission to reproduce figures and/or text from this article

[View the Full Text HTML](#)



**ACS Publications**  
High quality. High impact.

## GENERAL RESEARCH

## Mass Transfer in a Rotating Packed Bed with Viscous Newtonian and Non-Newtonian Fluids

Yu-Shao Chen,<sup>†</sup> Chia-Chang Lin,<sup>‡</sup> and Hwai-Shen Liu<sup>\*,†</sup>*Department of Chemical Engineering, National Taiwan University, Taipei, Taiwan, ROC, and  
Department of Chemical and Materials Engineering, Chang-Gung University, Tao-Yuan, Taiwan, ROC*

A theoretical analysis was developed to predict the apparent viscosity of a non-Newtonian fluid in a rotating packed bed. It is based on laminar liquid film flow on a rotating disk with the assumption of the randomly inclined surfaces in the rotating packed bed. In addition, experiments of deoxygenation were performed in glycerol solutions and CMC solutions, which are Newtonian and shear-thinning fluids, respectively. It is shown that mass transfer coefficients decreased with increasing viscosity, while the centrifugal force still revealed effective in enhancing mass transfer in viscous media. A correlation for mass transfer coefficient was proposed and valid for both the Newtonian and non-Newtonian fluids. Compared with a packed column, the influence of mass transfer coefficients by liquid viscosity was less in a rotating packed bed.

## Introduction

A rotating packed bed (i.e., Hige system), which replaces gravity with centrifugal force up to several hundred gravitational values, was introduced as a novel gas/liquid contactor to enhance mass transfer in 1981.<sup>1</sup> The system can be operated in higher ratios of gas/liquid flow rates due to the low tendency of flooding. Under a centrifugal field, thin liquid films and tiny liquid droplets are generated, which result in a decrease in mass transfer resistance and an increase in gas/liquid interfacial area. An 1 to 2 orders of enhancement in mass transfer can thus be achieved in a rotating packed bed. Consequently, the size and the capital of the processing system would be extremely reduced. The enhancement of mass transfer on gas/liquid and liquid/solid systems has been demonstrated in the literature.<sup>1–7</sup>

Some investigators have reported the correlations for the mass transfer coefficient in a rotating packed bed; however, studies of the effect of liquid viscosity on mass transfer in a rotating packed bed are lacking. For example, in 1985, Tung and Mah<sup>8</sup> proposed a correlation for a liquid-side mass transfer coefficient,  $k_L$ , based on the penetration theory and a developed laminar flow film model without considering the Coriolis force and the effect of the packing geometry. In 1989, Munjal et al.<sup>2</sup> proposed a correlation for  $k_L$  based on the developed laminar film flow on a rotating disk and on a rotating blade. In addition, Singh et al.<sup>9</sup> presented an empirical equation for the area of a transfer unit,  $ATU (= Q_L/zK_La)$ . The results showed that  $K_La$  was proportional to liquid viscosity to a power of 0.3, which is intuitively controversial. Though liquid viscosity was included in these correlations, a reasonable range of viscosity was

not experimentally investigated in these studies. Therefore, a systematic study of the influence of liquid viscosity on mass transfer in a rotating packed bed is needed.

Mass transfer in packed columns has been well-studied for several decades. Various correlations to predict a mass transfer coefficient in packed columns are available in the literature. However, most investigations employed water as the irrigating medium, and the correlations in the literature pertaining to the influence of the viscosity of the liquid phase on the mass transfer coefficient have shown considerable discrepancy. Therefore, in 1980, Mangers and Ponter<sup>10</sup> measured the absorption rate of carbon dioxide into pure water and aqueous glycerol mixtures (Newtonian fluids), covering a viscosity range of 0.9 to 26 cP in a packed column. They found that the volumetric liquid side mass transfer coefficient,  $k_La$ , decreased with increasing liquid viscosity. In 1991, Delaloye et al.<sup>11</sup> performed an experiment of deoxygenation in aqueous glycerol solution, viscosity ranging from 0.8 to 10 cP, in a packed column. A correlation of  $k_La$  with diffusivity of solute, liquid flow rate, and viscosity was developed.

$$\frac{k_La}{D^{0.5}} = 90L^{0.74}\mu^{-0.5} \quad (1)$$

According to these investigations, it is found that the mass transfer coefficient decreases as the viscosity of the liquid phase increases.

In addition, many industrial processes, such as stripping solvent and monomer from polymer solution and oxygen transfer in fermentation solution, are performed in viscous media, which very often behave as non-Newtonian fluids. For a shear-thinning fluid, the apparent viscosity would be reduced under high shear stress. Consequently, a rotating packed bed would be expectedly applicable in handling these viscous fluids

\* To whom correspondence should be addressed. Tel.: +886-2-3366-3050. Fax: +886-2-2362-3040. E-mail: hslu@ntu.edu.tw.

<sup>†</sup> National Taiwan University.

<sup>‡</sup> Chang-Gung University.

effectively. Therefore, in this study, the influence of the viscosity of the viscous Newtonian and non-Newtonian fluids on mass transfer was investigated in a rotating packed bed. For a non-Newtonian fluid, the apparent viscosity is a key parameter to predict mass transfer. Moreover, because it is difficult to directly measure the apparent viscosity in a rotating packed bed, a theoretical analysis was developed to predict the apparent viscosity of a non-Newtonian fluid in a rotating packed bed. In addition, experimental measurement of the mass transfer coefficient in a rotating packed bed was also carried out in glycerol solutions and CMC solutions, which are Newtonian and shear-thinning fluids, respectively.

## Theory

Some developments of mass transfer correlations for a rotating packed bed were based on the film flow assumption.<sup>2,8</sup> In addition, in 2000, Lin et al.<sup>12</sup> also presented a theoretical analysis of the liquid holdup in a rotating packed bed on the basis of the film flow on a rotating disk. On the other hand, in 1995, Basic and Dudukovic<sup>13</sup> experimentally measured the liquid holdup in a rotating packed bed to examine the film flow assumption. They found that the holdup could not be properly predicted on the basis of film flow. Burns and Ramshaw<sup>14</sup> and Guo et al.<sup>15</sup> reported visual studies of liquid flow in a rotating packed bed. Both of their results showed that the flow of liquid was more than the uniform film flow assumption. Though the models based on the film flow assumption did not have a strong physical basis, the results were shown to agree with experimental data.<sup>2,8,12</sup> Therefore, in this study, a model was proposed on the basis of film flow to estimate the apparent viscosity of a power-law fluid in a rotating packed bed.

For a power-law fluid, the apparent viscosity,  $\eta$ , can be calculated as<sup>16</sup>

$$\eta = K\dot{\gamma}^{n-1} \quad (2)$$

where  $K$  is the consistency index,  $n$  is the flow behavior index, and  $\dot{\gamma}$  is the shear rate, which can be expressed as

$$\dot{\gamma} = \sqrt{\frac{1}{2}(\Delta:\Delta)} \quad (3)$$

In eq 3,  $\Delta$  is the rate of the deformation tensor, defined as

$$\Delta = \nabla V + (\nabla V)' \quad (4)$$

where  $V$  is the velocity of the fluid, and  $(\nabla V)'$  represents the transpose of  $\nabla V$ .

The case of  $n = 1$  represents a Newtonian fluid with constant viscosity, whereas  $n < 1$  and  $n > 1$  correspond to the case of pseudoplastic (shear-thinning) and dilatant (shear-thickening) fluids, respectively. For a shear-thinning fluid ( $n < 1$ ), such as CMC solution, the apparent viscosity will decrease with increasing shear rate. This characteristic would make a rotating packed bed applicable.

**Film Flow on a Vertical Plane.** First, consider a laminar flow of a thin layer of a power-law fluid on a vertical plane. A coordinate system is defined with the  $x$  axis along the direction of gravity and the  $z$  axis

normal to the plane. The equation of motion for the liquid can be expressed as

$$\frac{\partial}{\partial z}\tau_{zx} = \rho g \quad (5)$$

where  $\tau_{zx}$  is shear stress for a power-law fluid and is defined as

$$\tau_{zx} = -K\left(\frac{dV_x}{dz}\right)^n \quad (6)$$

where  $V_x$  is the velocity in the  $x$  direction. The boundary conditions are given by at the plane surface ( $z = 0$ )

$$V_x = 0 \quad (7)$$

and at the free surface ( $z = h$ )

$$\tau_{zx} = 0 \quad (8)$$

According to eqs 5–8, the velocity profile of a power-law fluid on a vertical plane can be obtained

$$V_x = V_x^\infty \left[1 - \left(1 - \frac{z}{h}\right)^{(n+1)/n}\right] \quad (9)$$

where  $V_x^\infty$  is the free surface velocity defined as

$$V_x^\infty = \frac{n}{n+1} \left(\frac{\rho g}{K}\right)^{1/n} h^{(n+1)/n} \quad (10)$$

**Film Flow on a Rotating Disk.** The condition that liquid film flows on a rotating disk is considered, shown as Figure 1. The liquid velocity is assumed to be independent of  $\theta$ . The equations of continuity and motion for a power-law fluid may be written as

$$\frac{\partial V_r}{\partial r} + \frac{V_r}{r} + \frac{\partial V_z}{\partial z} = 0 \quad (11)$$

$$\rho \left( V_r \frac{\partial V_r}{\partial r} - \frac{V_\theta^2}{r} + V_z \frac{\partial V_r}{\partial z} \right) = -\frac{\partial}{\partial z}\tau_{zr} \quad (12)$$

$$\rho \left( V_r \frac{\partial V_\theta}{\partial r} + \frac{V_r V_\theta}{r} + V_z \frac{\partial V_\theta}{\partial z} \right) = -\frac{\partial}{\partial z}\tau_{z\theta} \quad (13)$$

where  $V_r$  is the velocity in the radial direction,  $V_\theta$  is the velocity in the tangential direction, and  $V_z$  is the velocity in the axial direction, which is perpendicular to the disk surface. Here,  $\tau_{zr}$  and  $\tau_{z\theta}$  are shear stress defined by

$$\tau_{zr} = -\eta \frac{\partial V_r}{\partial z} \quad (14)$$

$$\tau_{z\theta} = -\eta \frac{\partial V_\theta}{\partial z} \quad (15)$$

In eqs 12 and 13, the terms

$$\frac{1}{r} \frac{\partial}{\partial r}(r\tau_{rr}) \text{ and } \frac{1}{r^2} \frac{\partial}{\partial r}(r^2\tau_{r\theta})$$

have been omitted because these terms are an order of magnitude smaller than the terms on the right-hand side. In eqs 14 and 15,  $\eta$  is the apparent viscosity of a

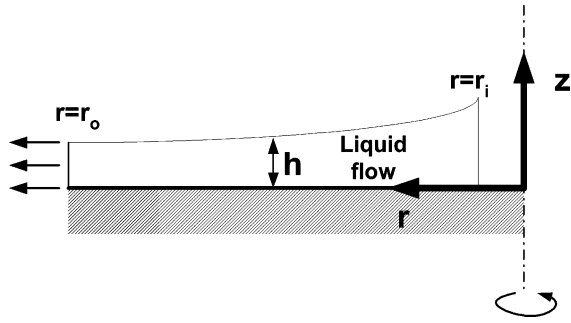


Figure 1. Schematic of flow over a rotating disk.

power-law fluid, and according to eq 2, it can be written as

$$\eta = K \left[ \left( \frac{\partial V_r}{\partial z} \right)^2 + \left( \frac{\partial V_\theta}{\partial z} \right)^2 \right]^{(n-1)/2} \quad (16)$$

The boundary conditions are given by the nonslip condition at the disk surface ( $z = 0$ )

$$V_r = 0 \quad (17a)$$

$$V_\theta = r\omega \quad (17b)$$

$$V_z = 0 \quad (17c)$$

and negligible shears at the free surface ( $z = h$ )

$$\tau_{zr} = 0 \quad (17d)$$

$$\tau_{z\theta} = 0 \quad (17e)$$

To overcome the difficulty of numerical computation, this problem should be simplified by assuming a velocity profile similar to that of the laminar film flow on a vertical plane, shown as eq 9.

$$V_r = V_r^\infty \left[ 1 - \left( 1 - \frac{z}{h} \right)^{(n+1)/n} \right] \quad (18)$$

$$V_\theta = V_\theta^\infty \left[ 1 - \left( 1 - \frac{z}{h} \right)^{(n+1)/n} \right] + r\omega \quad (19)$$

where  $V_r^\infty$  is the radial velocity at the free surface and only depends on  $r$ , and  $V_\theta^\infty$  is the tangential velocity at the free surface and also only depends on  $r$ . The volumetric liquid flow rate ( $Q_L$ ) can be expressed as

$$Q_L = 2\pi r \int_0^h V_r dz \quad (20)$$

Then, the thickness of the liquid film,  $h$ , can be obtained by integrating the above equation with the aid of eq 18.

$$h = \frac{(2n+1)Q_L}{(n+1)2\pi r V_r^\infty} \quad (21)$$

Since eqs 18 and 19 satisfy four boundary conditions (eqs 17a, 17b, 17d, and 17e), the axial velocity can be obtained by integrating eq 11 from 0 to  $z$  with eq 17c.

$$V_z = -\int_0^z \left( \frac{\partial V_r}{\partial r} + \frac{V_r}{r} \right) dz \quad (22)$$

Substituting eqs 18, 19, and 22 into eqs 12 and 13 and

integrating the resulting equations with respect to  $z$  between  $z = 0$  and  $z = h$  gives the following equations for the velocities at the liquid free surface.

$$\frac{dV_r^\infty}{dr} = \frac{V_\theta^\infty}{r V_r^\infty} + \frac{3n+2}{n+1} \frac{V_\theta^\infty \omega}{V_r^\infty} + \frac{(2n+1)(3n+2)r\omega^2}{2(n+1)^2 V_r^\infty} - \frac{(2n+1)(3n+2) \left( \frac{n+1}{n} \right)^n \frac{K}{\rho h^2} \left[ \left( \frac{V_r^\infty}{h} \right)^2 + \left( \frac{V_\theta^\infty}{h} \right)^2 \right]^{(n-1)/2}}{2(n+1)^2} \quad (23)$$

$$\frac{dV_\theta^\infty}{dr} = -\frac{V_\theta^\infty}{r} - \frac{3n+2}{n+1} \omega - \frac{(2n+1)(3n+2) \left( \frac{n+1}{n} \right)^n \frac{K}{\rho h^2} \frac{V_\theta^\infty}{V_r^\infty} \left[ \left( \frac{V_r^\infty}{h} \right)^2 + \left( \frac{V_\theta^\infty}{h} \right)^2 \right]^{(n-1)/2}}{2(n+1)^2} \quad (24)$$

Equations 23 and 24 can be solved numerically with the initial conditions that  $V_r^\infty = V_{r,i}^\infty$  and  $V_\theta^\infty = V_{\theta,i}^\infty$  at  $r = r_i$  to obtain the values of  $V_r^\infty$  and  $V_\theta^\infty$ . Then the velocity profile of a power-law liquid film on a rotating disk can be obtained by eqs 18 and 19.

Substituting the velocity components,  $V_r$  and  $V_\theta$ , into eq 16, the apparent viscosity, which depends on  $r$  and  $z$ , can thus be evaluated. For a convenient expression of the viscosity, the mean apparent viscosity in the  $z$ -direction,  $\eta_r$ , which only depends on  $r$ , is defined as

$$\eta_r = \frac{1}{h} \int_0^h \eta dz \quad (25)$$

Substituting eq 16 along with eqs 18 and 19 into above equation,  $\eta_r$  can be expressed as

$$\eta_r = K \left( \frac{n+1}{n} \right)^{n-1} \left( \frac{n}{2n-1} \right) \left[ \left( \frac{V_r^\infty}{h} \right)^2 + \left( \frac{V_\theta^\infty}{h} \right)^2 \right]^{(n-1)/2} \quad (26)$$

The mean apparent viscosity in the  $z$  direction of a shear-thinning fluid ( $n = 0.8$ ) along the radial direction on a rotating disk for two different initial radial velocities is shown in Figure 2. It is noted that  $\eta_r$  decreases along the radial distance. This can be explained by the fact that, in the outer region, the liquid is under a stronger shear stress as centrifugal force increases with radial distance.

In addition, an approximate analytical expression for the apparent viscosity is developed. It is assumed that  $dV_r^\infty/dr = 0$  and  $V_\theta^\infty = 0$ , and that eq 23 can be reduced to

$$V_r^\infty = \left[ \left( \frac{n+1}{n} \right)^n \frac{K}{\rho} \frac{1}{r\omega^2} \right]^{-1/n} h^{(n+1)/n} \quad (27)$$

Then substituting eq 27 into eq 21, we get

$$h = \left[ \left( \frac{2n+1}{n} \right)^n \left( \frac{Q_L}{2\pi r} \right)^n \frac{K}{\rho} \frac{1}{r\omega^2} \right]^{1/(2n+1)} \quad (28)$$

The approximate analytical expression of  $\eta_r$  is then

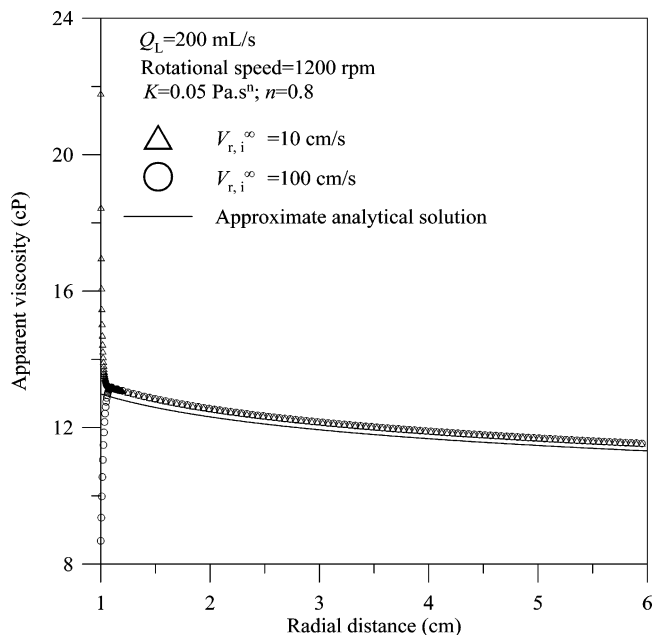


**Figure 2.** Apparent viscosity distributions on a rotating disk for different initial conditions.

obtained by substituting the assumption of  $V_{\theta}^{\infty} = 0$ , eqs 27 and 28, into eq 26.

$$\eta_r = K \left( \frac{n}{2n-1} \right) \left[ \left( \frac{2n+1}{n} \right)^{1/(2n+1)} \left( \frac{Q_L}{2\pi r} \right)^{1/(2n+1)} \times \left( \frac{K}{\rho} \right)^{-2/(2n+1)} \left( \frac{1}{r\omega^2} \right)^{-2/(2n+1)} \right]^{n-1} \quad (29)$$

The results of the approximate solution are shown as solid lines in Figure 2. It has been found that the viscosity predicted by the two different methods started with different values, whereas the initial condition does not influence the approximate solution. Although the apparent viscosity calculated by eq 26 depends on the initial velocity of liquid, it is clearly seen that the apparent viscosity is not very sensitive to the initial condition, except in the short entrance region. The viscosity predicted by both methods would approach a similar value at a distant radial location.

**Flow in a Rotating Packed Bed.** In 1959, Davidson<sup>17</sup> used a statistical model to extend the theoretical  $k_L$  expression for gravity film flow on a flat surface to a correlation for the packed bed. He assumed that the packing consists of a large number of surfaces randomly inclined at  $\theta$  to the horizontal, each of length  $d$  in the direction of flow, and of effective width  $b$ . According to these assumptions, the mean centrifugal field in which liquid flows in a rotating packed bed can be expressed as

$$a_c = \frac{2}{\pi} \int_0^{\pi/2} r\omega^2 \cos \theta d\theta \quad (30)$$

In addition, it is assumed that there are  $p$  surfaces per unit area in a rotating packed bed. Now considering a differential volume with cross-sectional area  $2\pi rz$  and thickness

$$\frac{2}{\pi} \int_0^{\pi/2} d \cos \theta d\theta$$

which is the average length of the surfaces in radial

direction, the surface area per unit volume can be expressed as

$$a = \frac{(2\pi rzp)bd}{2\pi rz \frac{2}{\pi} \int_0^{\pi/2} d \cos \theta d\theta} = \frac{\pi pb}{2} \quad (31)$$

and the liquid flow rate per unit width in a rotating packed bed,  $Q_w$ , can be obtained with the aid of eq 31.

$$Q_w = \frac{Q_L}{2\pi rzpb} = \frac{Q_L}{4rza} \quad (32)$$

The correlation of apparent viscosity for a rotating packed bed can be developed starting from eq 29. The terms of  $r\omega^2$  and  $Q_L/2\pi r$  in the equation are replaced by eqs 30 and 32, respectively, and for the randomly inclined surfaces, the apparent viscosity can be expressed as

$$\eta_{r,RPB} = K \left( \frac{n}{2n-1} \right) \left[ \left( \frac{2n+1}{n} \right)^{1/(2n+1)} \left( \frac{Q_L}{4rza} \right)^{1/(2n+1)} \times \left( \frac{K}{\rho} \right)^{-2/(2n+1)} \left( \frac{1}{a_c} \right)^{-2/(2n+1)} \right]^{n-1} \quad (33)$$

Because  $\eta_{r,RPB}$  varies along the radial direction in a rotating packed bed, it is useful to define a mean apparent viscosity for a rotating packed bed ( $\bar{\eta}_{RPB}$ ).

$$\bar{\eta}_{RPB} = \frac{1}{r_o^2 - r_i^2} \int_{r_i}^{r_o} \eta_{r,RPB} 2r dr \quad (34)$$

## Experimental Section

The main structure of a rotating packed bed is shown in Figure 3. The liquid enters the packed bed from a liquid distributor and sprays onto the inside edge of the packed bed. The liquid distributor has two vertical sets of holes in the opposite direction, and each set has three 0.5-mm-diameter holes. Then the liquid moves outward through the packing by the centrifugal force, is splashed onto the stationary housing, and is collected at the bottom. The gas is introduced from the stationary housing, flows inward through the packing, and leaves the rotor through the center pipe. Thus, the gas and the liquid contacts countercurrently in the rotating packed bed. The bed can be operated from 600 to 1500 rpm. The inner and outer radii of the bed were 1 and 6 cm, respectively, and the axial height of the bed was 2 cm. The bed was packed with 0.22-mm-diameter stainless steel wire meshes, whose porosity and interfacial area were 0.95 and 829 1/m, respectively.

Figure 4 shows a diagram of the experimental setup. Fresh liquid at a temperature of 30 °C was pumped into the rotating packed bed. A nitrogen stream with a flow rate of 1 L/min was introduced into the bed and contacted countercurrently with liquid. The concentrations of dissolved oxygen (DO) in the inlet and outlet liquid streams were measured by a DO probe (Ingold, type 170).

Glycerol solutions were used as a Newtonian fluid with various viscosities. The composition and the physical properties of the solution are presented in Table 1. The viscosity of the solution was measured by a viscometer (Brookfield, model DV-II+). The diffusivity of oxygen in glycerol solutions was computed from the experimental diffusion coefficients reported by Jordan



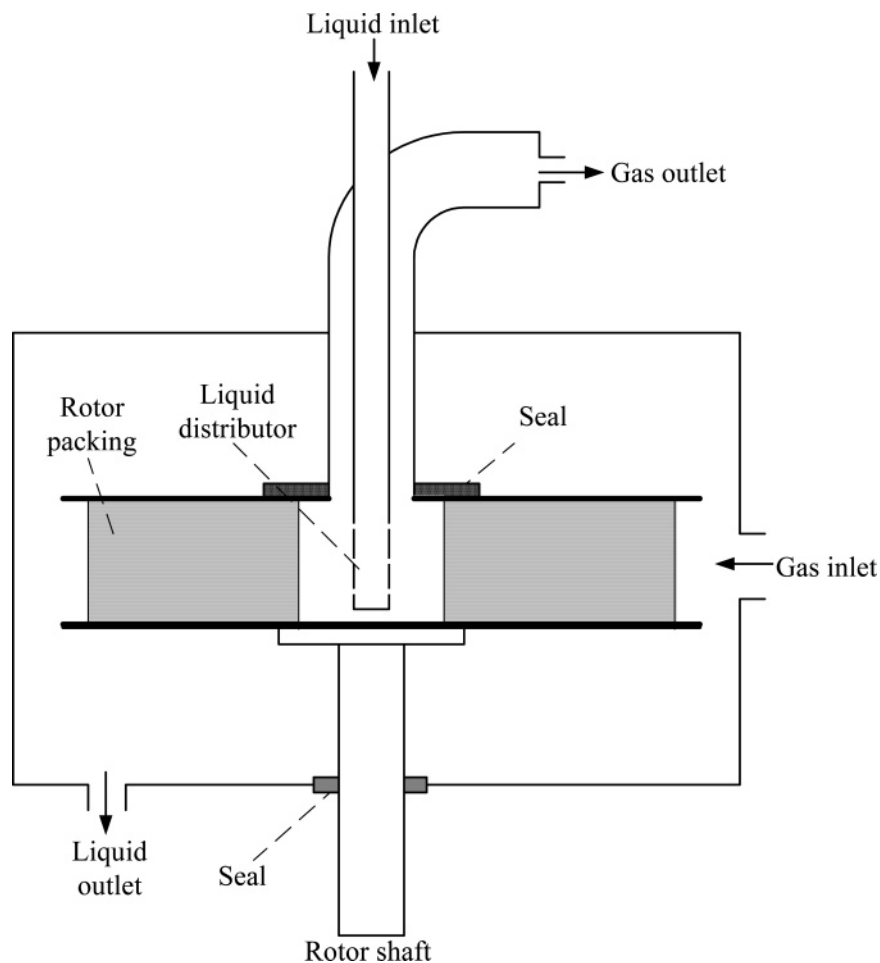


Figure 3. Main structure of a rotating packed bed.

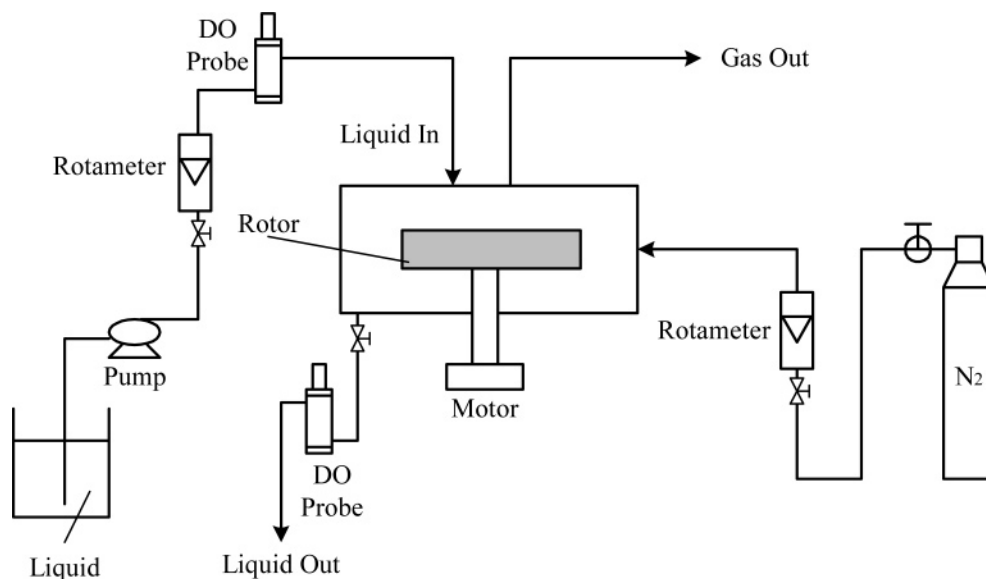


Figure 4. Diagram of the experimental setup.

et al.<sup>18</sup> The surface tension of the solution was evaluated from the experimental results of Mangers and Ponter<sup>10</sup> and Delaloye et al.<sup>11</sup> The density of glycerol solutions was from the data reported by Perry and Green.<sup>19</sup>

In addition to the Newtonian liquid, CMC solutions of different concentrations were proposed as a non-Newtonian fluids in the study. The rheological behavior of the CMC solutions was measured using a viscometer (Brookfield, model DV-II+). The values of the flow

behavior index ( $n$ ) and consistency index ( $K$ ) of CMC solutions of different concentration are listed in Table 2. Then the mean apparent viscosity ( $\bar{\eta}_{RPB}$ ) in a rotating packed bed for different operating conditions can be calculated using eq 34; the results are also shown in Table 2. The density and surface tension of the CMC solutions and the diffusivity of oxygen in the CMC solutions were approximately the same as those in water.<sup>20</sup>

**Table 1. Concentrations and Physical Properties of Glycerol Solutions**

glycerol concn (wt %)	$\mu$ (mPa s)	$\rho$ (kg/m <sup>3</sup> )	$\sigma$ (10 <sup>-3</sup> kg/s <sup>2</sup> )	$D$ (10 <sup>-9</sup> m <sup>2</sup> /s)
0	1.04	996	73.0	2.10
26	1.95	1059	71.5	2.26
46	3.98	1110	70.1	1.17
62	9.32	1154	68.6	0.94
68	14.4	1170	67.8	0.80
75	25.1	1189	66.9	0.59
80	40.5	1202	66.1	0.49

**Table 2. Rheological Parameters of CMC Solutions and the Apparent Viscosities by Theoretical Analysis**

CMC concn (wt %)	$K$ (Pa s <sup><i>n</i></sup> )	$n$	apparent viscosity, $\bar{\eta}_{RPB}$ (cP)			
			600 rpm	900 rpm	1200 rpm	1500 rpm
0.005	0.0014	0.9787	1.22	1.20	1.19	1.19
0.01	0.0026	0.9107	1.38	1.32	1.27	1.23
0.02	0.0058	0.8237	1.72	1.55	1.43	1.35
0.05	0.0194	0.7974	5.76	5.07	4.64	4.32
0.1	0.0526	0.8060	19.08	16.92	15.53	14.54
0.2	0.1036	0.7666	34.07	29.34	26.39	24.31
0.5	0.5670	0.7004	204.36	166.92	144.59	129.35

## Results and Discussion

To derive the design equation for a rotating packed bed, first consider a differential volume with cross-sectional area  $2\pi rz$  and thickness  $dr$ . Assuming that the gas-side mass transfer resistance can be neglected for the process of deoxygenation, then the mass balance of solute in this volume for a dilute system is

$$Q_L dx = k_L a (x^* - x) 2\pi r z dr \quad (35)$$

where  $x$  is mole fraction of solute (oxygen) in liquid phase,  $k_L a$  is the mass transfer coefficient, and  $x^*$  is the equilibrium concentration associated with the gas concentration. The overall mass balance is

$$Q_L(x - x_o) = Q_G(y - y_i) = Q_G(Hx^* - 0) \quad (36)$$

i.e.,

$$x^* = \frac{1}{S}(x - x_o) \quad (37)$$

where  $Q_G$  is gas flow rate;  $H$  is Henry's constant;  $x_o$  is the outlet dissolved oxygen concentration in the liquid;  $y_i$  is the inlet oxygen concentration in the gas; and  $S$  is stripping factor, defined as

$$S = \frac{HQ_G}{Q_L} \quad (38)$$

Then the mass transfer coefficient can be obtained by substituting eq 37 into eq 35 and integrating the equation from  $r = r_i$  to  $r = r_o$  with the boundary conditions  $x = x_i$  and  $x = x_o$ , respectively.

$$k_L a = \frac{Q_L}{\pi(r_o^2 - r_i^2)z} \frac{\ln\left[1 - \frac{1}{S}\frac{x_i}{x_o} + \frac{1}{S}\right]}{1 - \frac{1}{S}} \quad (39)$$

This equation is similar to that proposed by Singh et al.<sup>9</sup>

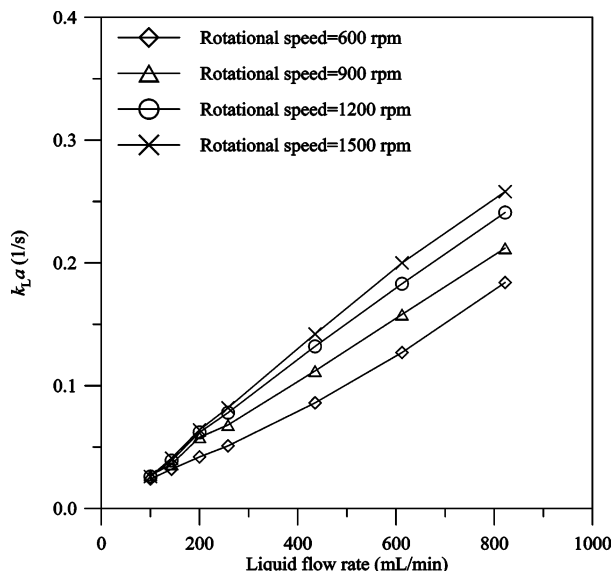


**Figure 5.** Dependence of  $k_L a$  in water on liquid rate at various rotational speeds.

Figure 5 shows  $k_L a$  values in water as a function of the liquid flow rate for four different rotational speeds. As expected, increasing the liquid rate increased the  $k_L a$  value. This observation is similar to that for a packed column. In addition, it is also found that  $k_L a$  increased as the rotational speed increased, indicating that the mass-transfer resistance was reduced with an increase in centrifugal force. However, the  $k_L a$  value does not significantly vary with rotational speed at a low liquid rate. The reason for this phenomenon may be that at a low liquid rate, most of the bed is not irrigated by liquid, and a severe channeling of the gas and the liquid may occur. Under this condition, only limited improvement on the maldistribution of liquid could be achieved by increasing the rotational speed.

For glycerol solutions that were the viscous Newtonian fluids, the viscosities ranging from 1 to 40.5 cP and liquid flow rates of 143 and 258 mL/min were investigated. Figure 6 shows the dependence of  $k_L a$  on the liquid viscosity for various rotational speeds. It is clear in the figure that  $k_L a$  decreases as the viscosity increases. This characteristic is similar to the results in a packed column.<sup>10,11</sup> An increase in liquid viscosity will lead to a slower flow of the liquid, a smaller degree of liquid mixing at the packing junction, and thicker liquid films, which cause the decrease in mass transfer efficiency. For example, when the liquid rate and the rotational speed were 258 mL/min and 1500 rpm, respectively, the residence time of the liquid would increase from 0.10 s to 0.34 s as the viscosity increased from 1 to 40.5 cP. However, it is also noted in Figure 6 that the mass transfer coefficient increased with increasing rotational speed for all the viscosities. It has been proven that the mass transfer efficiency can be intensified by centrifugal force when water is the irrigating medium. For the viscous media used in this study, it is further shown that the centrifugal force could also reduce mass transfer resistance effectively.

Figure 7 shows the  $k_L a$  value as a function of the rotational speed for various CMC concentrations (non-Newtonian fluid) at a liquid rate of 200 mL/min. It is shown in the Figure that the concentration of CMC solution has a significant effect on  $k_L a$ . The apparent viscosity of these non-Newtonian solutions can be

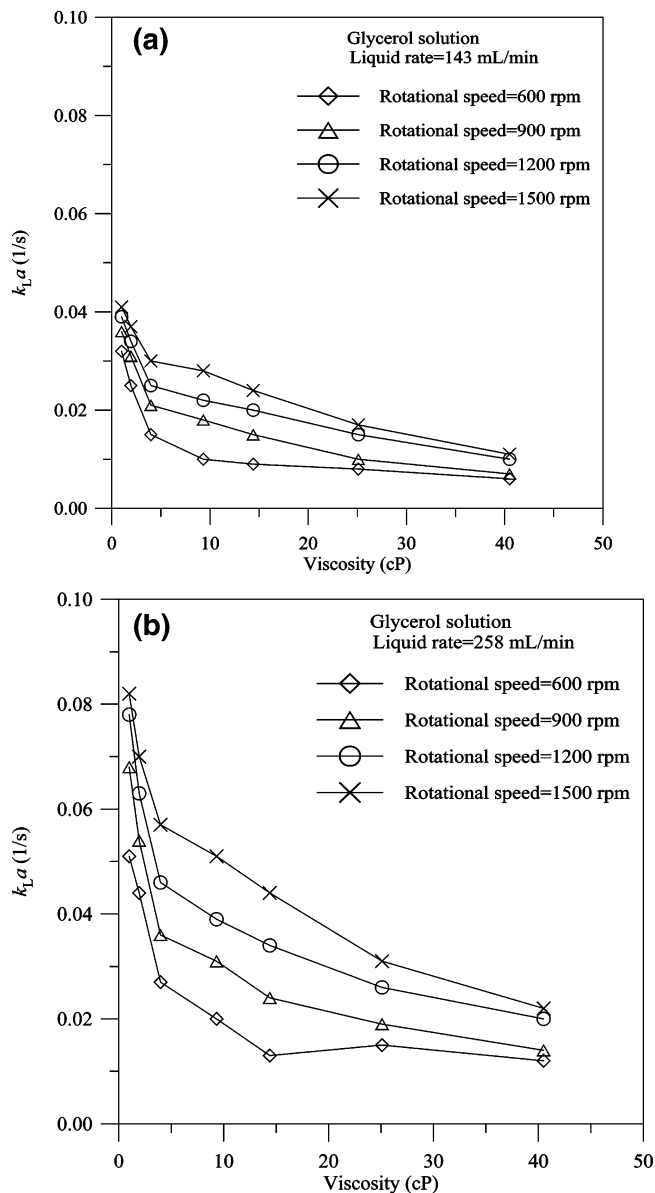


**Figure 6.** Dependence of  $k_L a$  in glycerol solutions on liquid viscosity at various rotational speeds at a liquid rate of (a) 143 mL/min and (b) 258 mL/min.

calculated by eq 34 with the help of the rheological properties listed in Table 2. The apparent viscosity in a rotating packed bed was found to increase with increasing concentration of the CMC solution and decrease with increasing rotational speed. The decrease of the apparent viscosity was more obvious for the fluid with small  $n$  value. For example, a 37% reduction of the apparent viscosity was achieved for 0.5% CMC solution as the rotational speed increased from 600 to 1500 rpm. On the basis of the apparent viscosity of the CMC solutions listed in Table 2, it can be seen that the  $k_L a$  decreased with increasing apparent viscosity. This characteristic indicates that the effect of the apparent viscosity of a non-Newtonian fluid on mass transfer may be similar to that of the viscosity of a Newtonian fluid on mass transfer.

A correlation of  $k_L a$  for both viscous Newtonian and non-Newtonian fluids was presented in eq 40 from the experimental results shown in Figures 5–7 with the

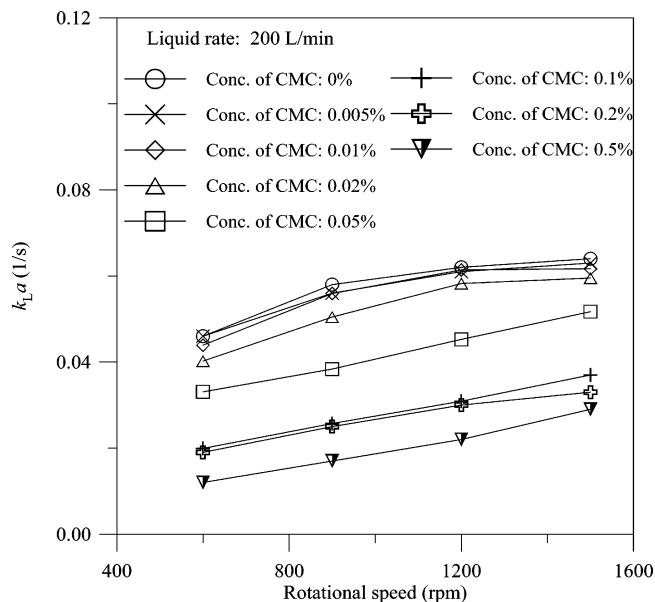


**Figure 7.** Dependence of  $k_L a$  in CMC solutions on rotational speed at various CMC concentrations.

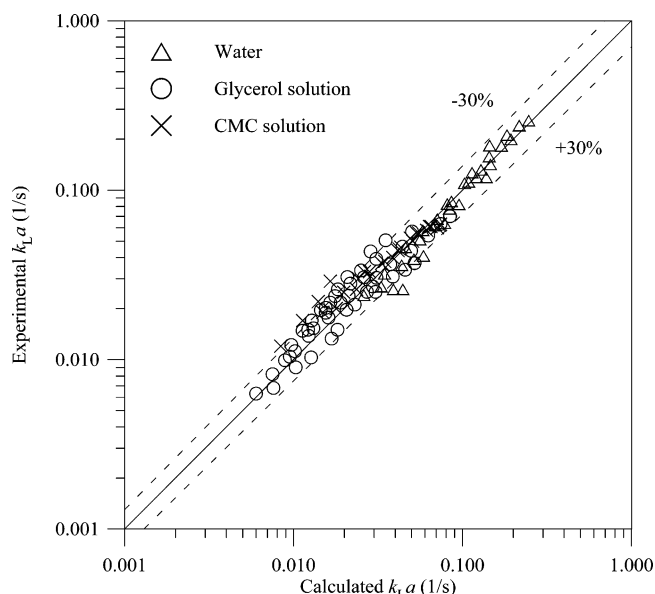


**Figure 8.** Comparison of experimental values of  $k_L a$  with results calculated using eq 40.

apparent viscosities of the CMC solutions predicted by theoretical analysis shown in Table 2.

$$\frac{k_L a d_p}{Da_t} = 0.9 Sc^{0.5} Re^{0.24} Gr^{0.29} We^{0.29} \quad (40)$$

In the equation,  $d_p$  is the spherical equivalent diameter of the packing,  $Sc$  is the Schmidt number,  $Re$  is the Reynolds number,  $Gr$  is the Grashof number, and  $We$  is the Weber number. As shown in Figure 8, most of the experimental results lie within  $\pm 30\%$  of the values estimated by eq 40. This result suggests that the correlation is valid for both Newtonian and non-Newtonian liquid systems, in which the apparent viscosity of a non-Newtonian fluid is estimated by the theoretical analysis on the basis of the film flow in a rotating packed bed.

From eq 40, it is found that  $k_L a$  is proportional to the liquid viscosity to the power of  $-0.32$ . Comparing with



the result reported by Delaloye et al.<sup>11</sup> for a packed column, shown as eq 1, less influence of liquid viscosity on mass transfer was obtained in a rotating packed bed than in a packed column. On the other hand, for a shear-thinning fluid, the apparent viscosity can be further decreased under a centrifugal field. As the result, a rotating packed bed is believed to be capable of handling the viscous Newtonian fluids and shear-thinning fluids.

## Conclusion

Though liquid viscosity was included in some correlations for mass transfer in a rotating packed bed, the effect of liquid viscosity on mass transfer has not been actually investigated. Therefore, this study performed experiments of deoxygenation in viscous Newtonian fluids and shear-thinning fluids in a rotating packed bed to investigate the influence of liquid viscosity on mass transfer. The apparent viscosity of the shear-thinning fluid in the bed is an unknown parameter and should be determined first. A theoretical analysis was developed to predict the apparent viscosity of a power-law fluid in a rotating packed bed. It is based on the laminar liquid film flow on a rotating disk, assuming that the velocity distribution is similar to that on a vertical plane. This analysis was further extended to a correlation for a rotating packed bed on the basis of a statistical model proposed by Davidson.<sup>16</sup> With the rheological properties of the solutions, the apparent viscosity in a rotating packed bed could be calculated for different operating conditions. According to the results of our experiments, it is clear that centrifugal force intensifies mass transfer in viscous media. In addition, a correlation for  $k_{1a}$  in the rotating packed bed was proposed. It is noted that the correlation is valid for both viscous Newtonian fluids and non-Newtonian fluids, and the dependence of  $k_{1a}$  on liquid viscosity is found less in a rotating packed bed than in a packed column.

## Acknowledgment

Financial support from the Ministry of Economic Affairs, Taiwan, ROC, is greatly appreciated.

## Nomenclature

$a$  = gas–liquid interfacial area (1/m)  
 $a_c$  = centrifugal acceleration (m/s<sup>2</sup>)  
 $a_t$  = surface area of the packing (1/m)  
 $b$  = effective width of packing surface (m)  
 $D$  = diffusion coefficient (m<sup>2</sup>/s)  
 $d$  = length of the packing surface (m)  
 $d_p$  = spherical equivalent diameter of the packing =  $6(1 - \epsilon)/a_t$  (m)  
 $g$  = gravitational force (m/s<sup>2</sup>)  
 $H$  = Henry's law constant  
 $h$  = liquid film thickness (m)  
 $K$  = consistency index (Pa s <sup>$n$</sup> )  
 $k_{1a}$  = volumetric mass transfer coefficient (1/s)  
 $L$  = liquid mass flux [kg/(m<sup>2</sup>s)]  
 $n$  = flow behavior index  
 $p$  = number of surfaces per unit area in a rotating bed  
 $Q_G$  = gas flow rate (m<sup>3</sup>/s)  
 $Q_L$  = liquid flow rate (m<sup>3</sup>/s)  
 $Q_w$  = liquid rate per unit width in a rotating packed bed (m<sup>2</sup>/s)  
 $r_i$  = inner radius of the packed bed (m)  
 $r_o$  = outer radius of the packed bed (m)  
 $S$  = stripping factor defined as eq 38

$V$  = velocity of fluid (m/s)  
 $V_r$  = velocity in the radial direction (m/s)  
 $V_r^\infty$  = radial velocity at the gas–liquid surface (m/s)  
 $V_{r,i}^\infty = V_r^\infty$  at  $r = r_i$  (m/s)  
 $V_x$  = velocity along the direction of gravity on a vertical surface (m/s)  
 $V_x^\infty = V_x$  at the gas–liquid surface (m/s)  
 $V_z$  = velocity in the axial direction (m/s)  
 $V_\theta$  = velocity in the tangential direction (m/s)  
 $V_\theta^\infty$  = tangential velocity at the gas–liquid surface relative to the disk surface (m/s)  
 $V_{\theta,i}^\infty = V_\theta^\infty$  at  $r = r_i$  (m/s)  
 $x$  = mole fraction of solute in liquid stream  
 $x^*$  = equilibrium concentration associated with the gas concentration  
 $x_i$  = mole fraction of solute in the inlet liquid stream  
 $x_o$  = mole fraction of solute in the outlet liquid stream  
 $y$  = mole fraction of solute in gas stream  
 $y_i$  = mole fraction of solute in the inlet gas stream  
 $z$  = axial height of the packing (m)

## Greek Letters

$\Delta$  = rate of deformation tensor (1/s)  
 $\dot{\gamma}$  = shear rate (1/s)  
 $\epsilon$  = porosity of the packing  
 $\eta$  = apparent viscosity (Pa s)  
 $\bar{\eta}_{\text{RPB}}$  = mean apparent viscosity in a rotating packed bed defined by eq 34 (Pa s)  
 $\eta_r$  = mean apparent viscosity in  $z$  direction (Pa s)  
 $\eta_{r,\text{RPB}}$  = mean apparent viscosity in  $z$  direction in a rotating packed bed (Pa s)  
 $\theta$  = angle of packing surface to the horizontal (rad)  
 $\mu$  = viscosity (mPa s)  
 $\rho$  = density (kg/m<sup>3</sup>)  
 $\sigma$  = surface tension (kg/s<sup>2</sup>)  
 $\tau$  = shear stress (Pa)  
 $\omega$  = rotational speed (rad/s)

## Dimensionless Groups

$Gr$  = Grashof number =  $d_p^3 a_c \rho^2 / \mu^2$   
 $Re$  = Reynolds number =  $L / a_t \mu$   
 $Sc$  = Schmidt number =  $\mu / \rho D$   
 $We$  = Weber number =  $L^2 / \rho a_t \sigma$

## Literature Cited

- (1) Ramshaw, C.; Mallinson, R. H. Mass Transfer Process. U.S. Patent 4,283,255, 1981.
- (2) Munjal, S.; Dudukovic, M. P.; Ramachandran, P. Mass-Transfer in Rotating Packed Beds—I. Development of Gas–Liquid and Liquid–Solid Mass-Transfer Correlations. *Chem. Eng. Sci.* **1989**, *44*, 2245.
- (3) Munjal, S.; Dudukovic, M. P.; Ramachandran, P. Mass-Transfer in Rotating Packed Beds—II. Experimental Results and Comparison with Theory and Gravity Flow. *Chem. Eng. Sci.* **1989**, *44*, 2257.
- (4) Lin, C. C.; Liu, H. S. Adsorption in a Centrifugal Field: Basic Dye Adsorption by Activated Carbon. *Ind. Eng. Chem. Res.* **2000**, *39*, 161.
- (5) Chen, Y. S.; Liu, H. S. Absorption of Vocs in a Rotating Packed Bed. *Ind. Eng. Chem. Res.* **2002**, *41*, 1583.
- (6) Lin, C. C.; Ho, T. J.; Liu, W. T. Distillation in a Rotating Packed Bed. *J. Chem. Eng. Jpn.* **2002**, *35*, 1298.
- (7) Lin, C. C.; Liu, W. T.; Tan, C. S. Removal of Carbon Dioxide by Absorption in a Rotating Packed Bed. *Ind. Eng. Chem. Res.* **2003**, *42*, 2381.
- (8) Tung, H. H.; Mah, R. S. H. Modeling Liquid Mass Transfer in Hige Separation Process. *Chem. Eng. Commun.* **1985**, *39*, 147.
- (9) Singh, S. P.; Wilson, J. H.; Counce, R. M.; Villiersfisher, J. F.; Jennings, H. L.; Lucero, A. J.; Reed, G. D.; Ashworth, R. A.; Elliott, M. G. Removal of Volatile Organic Compounds from Groundwater Using a Rotary Air Stripper. *Ind. Eng. Chem. Res.* **1992**, *31*, 574.

- (10) Mangers, R. J.; Ponter, A. B. Effect of Viscosity on Liquid Film Resistance to Mass Transfer in a Packed Column. *Ind. Eng. Chem. Process Des. Dev.* **1980**, *19*, 530.
- (11) Delaloye, M. M.; Stockar, U. v.; Lu, X. P. The Influence of Viscosity on the Liquid-Phase Mass Transfer Resistance in Packed Columns. *Chem. Eng. J.* **1991**, *47*, 51.
- (12) Lin, C. C.; Chen, Y. S.; Liu, H. S. Prediction of Liquid Holdup in Countercurrent-Flow Rotating Packed Bed. *Trans. Inst. Chem. Eng. Part A* **2000**, *78*, 397.
- (13) Basic, A.; Dudukovic, M. P. Liquid Holdup in Rotating Packed-Beds—Examination of the Film Flow Assumption. *AIChE J.* **1995**, *41*, 301.
- (14) Burns, J. R.; Ramshaw, C. Process Intensification: Visual Study of Liquid Maldistribution in Rotating Packed Beds. *Chem. Eng. Sci.* **1996**, *51*, 1347.
- (15) Guo, K.; Guo, F.; Feng, Y. D.; Chen, J. F.; Zheng, C.; Gardner, N. C. Synchronous Visual and Rtd Study on Liquid Flow in Rotating Packed-Bed Contactors. *Chem. Eng. Sci.* **2000**, *55*, 1699.
- (16) Bird, R. B.; Stewart, W. E.; Lightfoot, E. N. *Transport Phenomena*; McGraw-Hill: New York, 1960.
- (17) Davidson, J. F. The Hold-Up and Liquid Film Coefficient of Packed Towers, Part II: Statistical Models of Random Packings. *Trans. Instn Chem. Eng.* **1959**, *37*, 131.
- (18) Jordan, J.; Ackerman, E.; Berger, R. L. Polarographic Diffusion Coefficients of Oxygen Defined by Activity Gradients in Viscous Media. *J. Am. Chem. Soc.* **1956**, *78*, 2979.
- (19) Perry, R. H.; Green, D. W. *Chemical Engineers' Handbook*, 6th ed.; McGraw-Hill: New York, 1984.
- (20) Anabtawi, M. Z.; Hilal, N.; Al Muftah, A. E. Volumetric Mass Transfer Coefficient in Non-Newtonian Fluids in Spout Fluid Beds—Part 1. *Chem. Eng. Technol.* **2003**, *26*, 759.

Received for review January 19, 2004

Revised manuscript received November 15, 2004

Accepted November 22, 2004

IE0499409